Available online at www.sciencedirect.com
SCIENCE DIRECT®
Journal of Power Sources 124 (2003) 533–537
JOURNAL OF POWER SOURCES
www.elsevier.com/locate/jpowsour

Short communication

Synthesis and electrochemical properties of layer-structured $0.5Li(Ni_{0.5}Mn_{0.5})O_2$–$0.5Li(Li_{1/3}Mn_{2/3})O_2$ solid mixture☆

S.-H. Kang*, K. Amine

Electrochemical Technology Program, Chemical Engineering Division, Argonne National Laboratory, Argonne, IL 60439, USA

Received 30 May 2003; accepted 21 June 2003

Abstract

A 1:1 mixture of electrochemically active $Li(Ni_{0.5}Mn_{0.5})O_2$ and electrochemically inactive $Li(Li_{1/3}Mn_{2/3})O_2$, i.e. $Li(Li_{0.17}Ni_{0.25}Mn_{0.58})O_2$, has been synthesized by a sol–gel method. The mixture was calcined at 900 °C in air for 24 h and cooled at three different rates: quenched into liquid nitrogen, 2 °C/min, and 0.5 °C/min. It was found that the crystallographic structure and electrochemical properties of $Li(Li_{0.17}Ni_{0.25}Mn_{0.58})O_2$ highly depend on the cooling rate. The sample quenched into liquid nitrogen exhibited a long irreversible plateau at ca. 4.5 V during the first charge, and the discharge capacity gradually increased from 170 to 210 mAh/g after 40 cycles. The samples cooled at slower rates exhibited more monoclinic character and cubic spinel phase was observed; they showed no plateaus at 4.5 V during the first charge and the discharge capacities also gradually increased from 80 and 55 mAh/g to 130 and 85 mAh/g for 2 and 0.5 °C/min-cooled samples, respectively.

Keywords: Li-ion secondary batteries; Layered structure; $Li(Li,Ni,Mn)O_2$; Quenching

1. Introduction

Recently, a concept of making solid solutions of two layered materials, $LiMO_2$ (M = Co, Cr, $Ni_{0.5}Mn_{0.5}$) and $Li(Li_{1/3}M'_{2/3})O_2$ (M′ = Mn, Ti), has been adopted to stabilize the structure and to improve the electrochemical properties of the layered cathode materials for rechargeable lithium batteries [1–5]. $Li(Li_{1/3}M'_{2/3})O_2$, which has monoclinic symmetry (*C*2/*m*) due to the ordered distribution of Li and Mn in the transition-metal layers [6], is electrochemically inactive because all of the M′ ions exist in the 4+ oxidation state so that no lithium can be extracted from the structure. Therefore, it is generally expected that $Li(Li_{1/3}M'_{2/3})O_2$ acts as an inert matrix in the solid solution so that the overall capacity is sacrificed with increasing amount of $Li(Li_{1/3}M'_{2/3})O_2$.

However, it has been shown that the role of $Li(Li_{1/3}M'_{2/3})O_2$ in the solid solution is more than that of a mere inert matrix. For example, solid solutions of $LiCrO_2$ with poor electrochemical properties and $Li(Li_{1/3}Mn_{2/3})O_2$ with no electrochemical activity have shown excellent electrochemical behavior, especially for $0.4LiCrO_2$–$0.6Li(Li_{1/3}Mn_{2/3})O_2$, i.e. $Li(Li_{0.2}Cr_{0.4}Mn_{0.4})O_2$, where the Cr^{3+}/Cr^{6+} redox couple is responsible for the lithium extraction/insertion [2]. A solid solution of $Li(Ni_{0.5}Mn_{0.5})O_2$ and $Li(Li_{1/3}Mn_{2/3})O_2$ is another good example. According to Lu and Dahn [7], the solid solution $(1-x)Li(Ni_{0.5}Mn_{0.5})O_2$–$xLi(Li_{1/3}Mn_{2/3})O_2$ with $1/6 \leq x \leq 1/3$ exhibited a long, irreversible plateau at near 4.6 V during the first charge, which is not present in other layered cathode materials such as $LiCoO_2$, $LiNiO_2$, and $Li(Ni_{0.5}Mn_{0.5})O_2$, and delivered much higher capacity than theoretical one based on the Ni^{2+}/Ni^{4+} redox couple. From an academic as well as a technological point of view, we believe that it is very interesting and important to explore the origins of the improved electrochemical properties of the $LiM'O_2$–$Li(Li_{1/3}Mn_{2/3})O_2$ (M′ = Cr, $Ni_{0.5}Mn_{0.5}$) solid solutions and the unique role of $Li(Li_{1/3}Mn_{2/3})O_2$ therein.

We have been investigating layered cathode materials that contain tetravalent Mn ion as a major constituent, such as $Li(Ni_{0.5-x}Mn_{0.5-x}A_{2x})O_2$ and $Li[Li_{(1/3-2x/3)}Ni_{x-y}Mn_{(2/3-x/3-z)}A_{y+z}]O_2$ (A = Al, Co, Mg, Ti) [8–10]. In this paper, we report the synthesis and electrochemical

☆ This paper has been created by the University of Chicago as Operator of Argonne National Laboratory (Argonne@) under Contract No. W-31-109-ENG-38 with the US Department of Energy. The US Government retains for itself, and others acting on its behalf, a paid-up, non-exclusive, irrevocable worldwide license in said article to reproduce, prepare derivative works, distribute copies to the public, and perform publicly and display publicly, by or on behalf of the government.

* Corresponding author. Tel.: +1-630-252-4212; fax: +1-630-252-4176.
E-mail address: kangs@cmt.anl.gov (S.-H. Kang).

0378-7753/$ – see front matter © 2003 Elsevier B.V. All rights reserved.
doi:10.1016/S0378-7753(03)00804-8

properties of the 1:1 mixture of $Li(Ni_{0.5}Mn_{0.5})O_2$ and $Li(Li_{1/3}Mn_{2/3})O_2$, i.e. $Li(Li_{0.17}Ni_{0.25}Mn_{0.58})O_2$. In particular, the effects of the cooling rate on the crystallographic structure and the cycling behavior are presented.

2. Experimental

$Li(Li_{0.17}Ni_{0.25}Mn_{0.58})O_2$ was prepared by a sol–gel method from $Li(CH_3COO)\cdot H_2O$, $Ni(CH_3COO)_2\cdot 4H_2O$, and $Mn(CH_3COO)_2\cdot 4H_2O$. Each of the starting materials was dissolved in distilled water and added to the glycolic/tartaric acid solution that was used as a chelating agent. The solution pH was adjusted to around 7 using ammonium hydroxide. The entire process was conducted under continuous stirring and heating on a hot plate. The resulting gel precursor was decomposed at 450 °C for 5 h in air. The decomposed powders were then fired at 900 °C for 24 h in air and cooled at three different rates: quenched into liquid nitrogen, 2 °C/min, and 0.5 °C/min, each of which will be referred to Q24, S24, and VS24, respectively, throughout this paper. The crystallographic structure of the synthesized materials was examined by a powder X-ray diffractometer (XRD) using Cu Kα radiation.

Galvanostatic charge/discharge cycling was conducted with coin cells that were prepared in a dry room. The positive electrode consisted of 70 wt.% oxide powder, 25 wt.% acetylene black, and 5 wt.% polytetrafluoroethylene (PTFE) binder and was pressed onto an aluminum mesh current collector. Metallic lithium was used as the negative electrode. The electrolyte was 1 M $LiPF_6$ in a 1:1 mixture of ethylene carbonate (EC)/diethyl carbonate (DEC); the separator was Celgard® 2500. The coin cells were galvanostatically cycled in the voltage range of 2.0–4.6 V at a current density of 0.1 mA/cm^2 (∼10 mA/g) at room temperature.

3. Results and discussion

XRD patterns of $Li(Li_{0.17}Ni_{0.25}Mn_{0.58})O_2$ calcined at 900 °C for 24 h and cooled at different rates are shown in Fig. 1. It is noted that there exist clear differences in the XRD patterns among the three samples. Most of the peaks in the XRD pattern of the Q24 sample could be indexed based on the α-$NaFeO_2$ structure ($R\bar{3}m$) with extra peaks between 20 and 30° (labeled with m) that are characteristics of monoclinic $Li(Li_{1/3}Mn_{2/3})O_2$ [6]. Lu et al. [3] attributed the small, extra peaks that appeared at ∼21° in the XRD patterns of $Li[Ni_xLi_{1/3-2x/3}Mn_{2/3-x/3}]O_2$ ($0 < x < 1/2$) to the ordering of Li and Mn in the transition-metal layers. There also appeared trace of peaks or small shoulders (marked with solid circles) at higher angle, which are observed more clearly in the slow-cooled samples as shown in Fig. 1(b) and (c). In the XRD patterns of $Li(Li_{0.17}Ni_{0.25}Mn_{0.58})O_2$ samples cooled at 2 °C/min (S24) and 0.5 °C/min (VS24), new peaks that were negligible or absent in the quenched sample

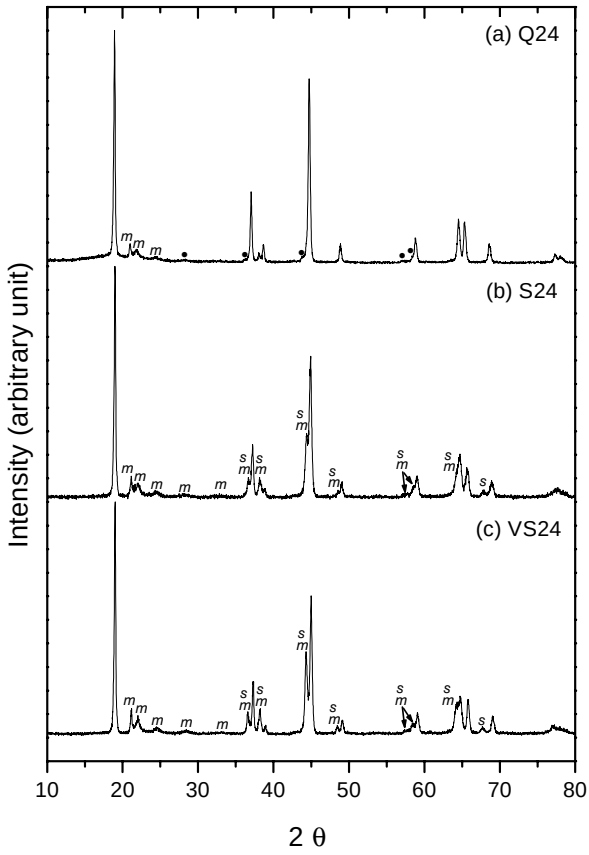

Fig. 1. XRD patterns of $Li(Li_{0.17}Ni_{0.25}Mn_{0.58})O_2$ calcined at 900 °C for 24 h in air and cooled at different rates: (a) quenched into liquid nitrogen; (b) 2 °C/min; and (c) 0.5 °C/min. The 'm' and 's' denote monoclinic and cubic spinel, respectively.

appeared over the whole 2θ range; the new peaks are more clearly resolved in the more slowly cooled sample (VS24). It is very hard to tell whether the new diffraction peaks represent monoclinic symmetry of $Li(Li_{1/3}Mn_{2/3})O_2$ or cubic symmetry of $Li_{1+y}Mn_{2-y}O_4$ except the ones at ∼33 and ∼67°; the former belongs only to monoclinic structure and the latter only to cubic spinel structure. Recently, Kim et al. [11] reported that they observed cubic spinel phase by TEM in $Li(Li_{0.1}Ni_{0.35}Mn_{0.55})O_2$ although the XRD pattern of the material did not reveal any diffraction peaks corresponding to cubic structure. The XRD patterns in Fig. 1 suggest the followings: (1) there exists partial ordering of Li and Mn (and/or Ni) in the transition-metal layer of the rhombohedral structure at 900 °C; (2) Li and transition-metals redistribute during slow cooling, which results in the formation of monoclinic and cubic spinel phases; (3) coexistence of rhombohedral, monoclinic, and cubic phases is thought to be thermodynamically favorable at room temperature in the one-to-one solid mixture of $Li(Ni_{0.5}Mn_{0.5})O_2$ and $Li(Li_{1/3}Mn_{2/3})O_2$.

Galvanostatic charge/discharge curves and the corresponding discharge capacities of the three samples cooled at the different rates are shown in Figs. 2 and 3, respectively.

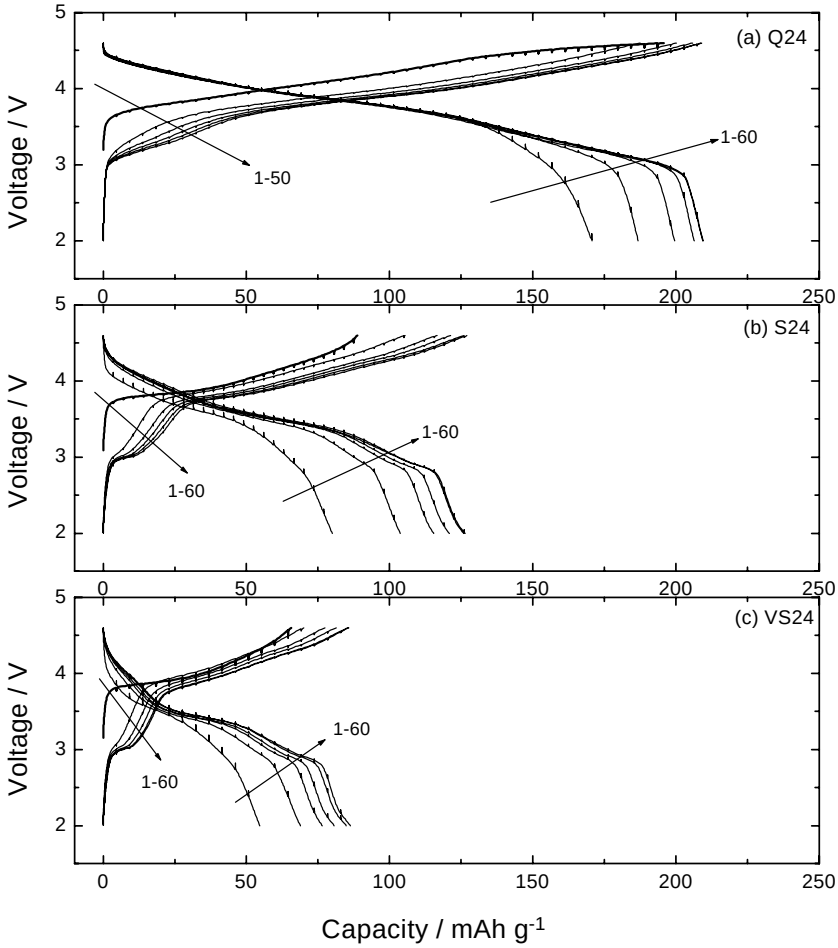

Fig. 2. Galvanostatic charge/discharge curves of (a) Li/Q24, (b) Li/S24, and (c) Li/VS24 cells cycled between 2.0 and 4.6 V at a current density of 0.1 mA/cm^2.

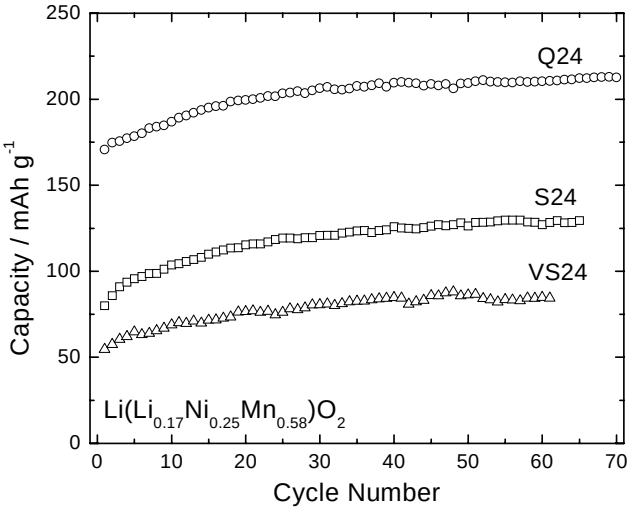

Fig. 3. Discharge capacities of Q24, S24, and VS24 in the voltage range of 2.0–4.6 V.

The initial discharge capacities of Q24, S24, and VS24 were 170, 80, and 55 mAh/g, respectively, and the subsequent capacities increased gradually with cycling and stabilized at 210, 130, and 85 mAh/g, respectively, after about 40th cycle.

The quenched sample (Q24) exhibited an irreversible plateau at 4.5–4.6 V during the first charge; the plateau started at the capacity close to a theoretical value for the reaction of $Li(Li^{+}_{0.17}Ni^{2+}_{0.25}Mn^{4+}_{0.58})O_2 \rightarrow Li_{0.5}(Li^{+}_{0.17}Ni^{4+}_{0.25}Mn^{4+}_{0.58})O_2 + 0.5Li$ (155 mAh/g). On the other hand, such high-voltage plateaus were not observed for the slow-cooled samples. The appearance of the plateau and the magnitude of capacity at the end of the first charge observed in the Q24 cathode are very puzzling because it is supposed that there is no more metal elements that can be oxidized further once the composition reaches $Li_{0.5}(Li^{+}{}_{0.17}Ni^{4+}{}_{0.25}Mn^{4+}{}_{0.58})O_2$. Lu and Dahn [7] reported similar plateaus at 4.5V during the first charge of $Li/Li[Ni_xLi_{1/3-2x/3}Mn_{2/3-x/3}]O_2$ ($1/6 = x = 12/5$) cells; they explained the plateaus in terms of irreversible oxygen loss. However, we consider that the amount of lost oxygen calculated by Lu et al. based on the length of the plateaus at 4.5 V is

too large; for example, $Li(Li_{0.222}Ni_{0.167}Mn_{0.611})O_2$ became $Li_x(Li_{0.222}Ni_{0.167}Mn_{0.611})O_{1.667}$, where $x = 0$ at the fully charged state and $x = 1$ after the subsequent discharge. It is questionable whether the material can keep the layered structure with that large oxygen deficiency. Participation of oxygen ions in the redox reactions can be another possible explanation on the charge compensation mechanism at voltage higher than 4.5 V during the first charge. Recently, it was reported that oxidation of oxide ions was partially responsible for charge compensation in $Li(Li_{0.15}Ni_{0.275-x}Mg_xMn_{0.575})O_2$ [12], $LiCo_{0.5}Ni_{0.5}O_2$ [13,14], and $LiAl_yCo_{1-y}O_2$ ($0 \leq y \leq 0.25$) [15,16].

Differential capacity versus voltage plots of the three samples are shown in Fig. 4. In Fig. 4(a), it is noticed that new differential capacity peaks develop at 3.2 V on charging (3.1 V on discharging) with cycling of the quenched sample, which is believed to be responsible for the capacity increase with cycling of the Q24 sample since the differential capacity plot does not change with cycling above 3.5 V after the first cycle. Lu and Dahn [7] attributed the differential capacity peaks below 3.5 V to participation of Mn ions in the redox reactions in the layered structure. The average voltage of the new differential capacity peaks (~3.15 V) is in between that of Mn^{3+}/Mn^{4+} couple in $LiMnO_2$ (~3.6 V) [17,18] and in $Li_{2/3}(Ni_{1/3}Mn_{2/3})O_2$ (~2.8 V) [19]. It is supposed that different ionic surroundings yielded different redox potentials in the similar structures. As is shown in Fig. 4(b) and (c), the slow-cooled samples exhibited much sharper differential capacity peaks centered at lower voltage (~2.95 V) than those of the quenched sample, which can be attributed to Mn^{3+}/Mn^{4+} couple with lithium insertion/extraction into/from octahedral sites in the spinel phase present in the slow-cooled samples as was observed in the XRD patterns.

Fig. 5 shows the XRD patterns of the cycled Q24 and VS24 samples. It is noted that the diffraction peaks at 20–25°

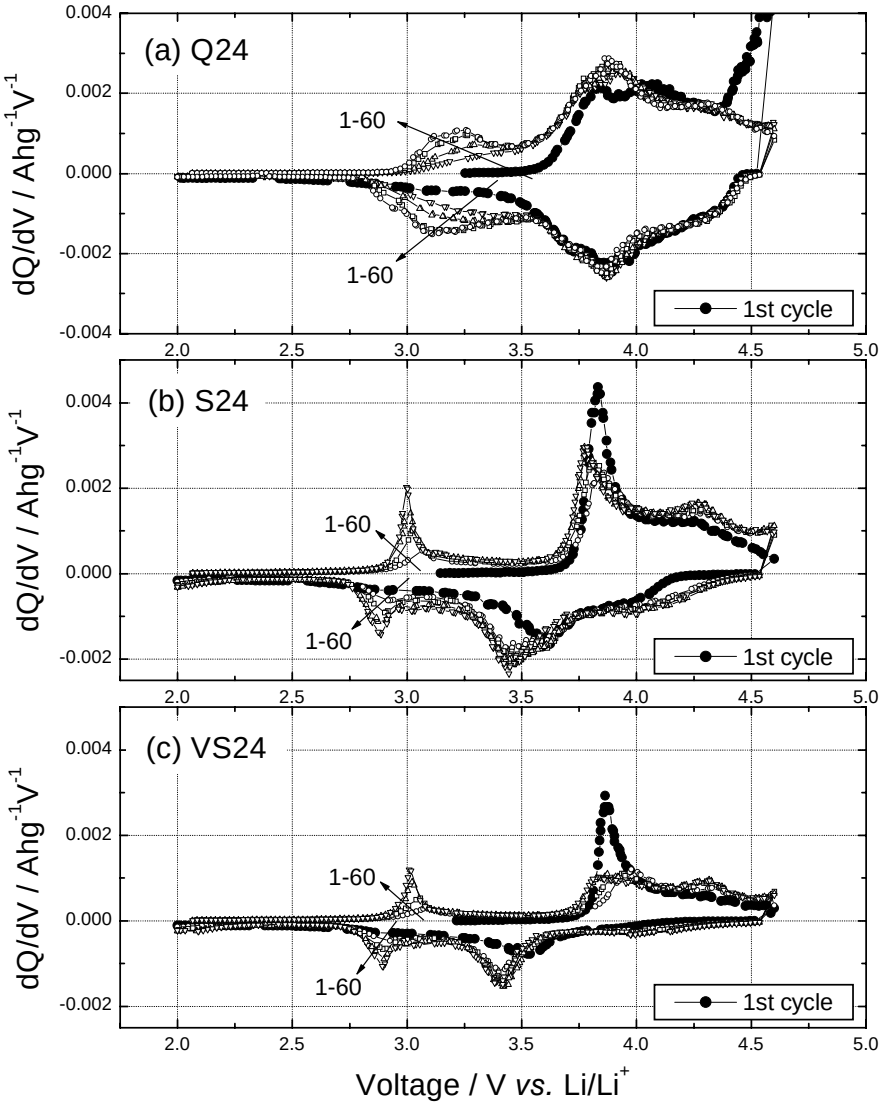

Fig. 4. Differential capacity vs. voltage plots of the cells (a) Li/Q24, (b) Li/S24, and (c) Li/VS24 cycled at 2.0–4.6 V. The number denotes cycle number of each cell.

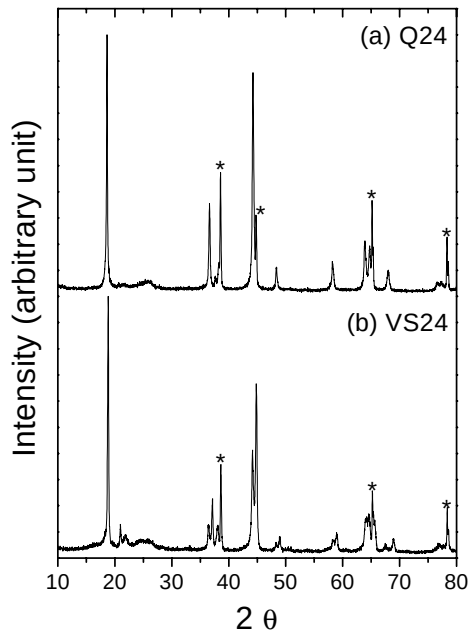

Fig. 5. XRD patterns of the Q24 and VS24 cathodes cycled between 2.0 and 4.6 V. Both of the cathodes were discharged to 2.0 V before the X-ray scanning. The peaks marked with asterisk are from aluminum current collector.

disappeared in the cycled Q24 cathode whereas those in the cycled VS24 cathode remained almost intact. As was discussed in our recent report [10], disappearance of the diffractions peaks at 20–25° in the cycled Q24 cathode suggests lithium removal from transition-metal layers during electrochemical cycling, especially during the 4.5 V plateau at the first charge. More works are under way to investigate the origin of disappearance of the diffraction peaks at 20–25° and its relation with the 4.5 V plateau during the first charge.

4. Summary and conclusions

Layered $Li(Li_{0.17}Ni_{0.25}Mn_{0.58})O_2$, which corresponds to a 1:1 solid mixture of $Li(Ni_{0.5}Mn_{0.5})O_2$ and $Li(Li_{1/3}Mn_{2/3})O_2$, was synthesized by a sol–gel method; the effect of the cooling rate after calcination (900 °C, 24 h, air) on the crystallographic structure and the electrochemical properties was investigated. The quenched material showed an α-$NaFeO_2$-type layered structure with a minor monoclinic character, whereas a greater degree of monoclinic character and cubic spinel phase were found in the slow-cooled materials. The electrochemical properties were also found to highly depend on the cooling rate; the quenched sample exhibited an irreversible plateau at ca. 4.5 V during the first charge cycle and delivered a discharge capacity of 210 mAh/g that is larger than the theoretical one (155 mAh/g) based on Ni^{2+}/Ni^{4+} redox couple. The slow-cooled samples did not exhibit the 4.5 V plateau and delivered much smaller discharge capacities than the quenched one. All of the three samples showed the evolution of differential capacity peaks near 3 V with cycling. The new differential capacity peak in the quenched sample centered on 3.15 V is supposed to be caused by Mn^{3+}/Mn^{4+} redox couple in the layered structure, whereas those in the slow-cooled samples centered on 2.95 V are attributed to Mn^{3+}/Mn^{4+} couple in the cubic spinel structure present in the slow-cooled samples as an impurity. The XRD patterns of the cycled cathodes revealed that Li-ions in the transition-metal layers were removed irreversibly during electrochemical cycling of the quenched sample.

More extensive and systematic studies are necessary to explore the peculiar and interesting electrochemical behavior of $Li(Ni_{0.5}Mn_{0.5})O_2$–$Li(Li_{1/3}Mn_{2/3})O_2$ solid mixture such as the 4.5 V plateau during the first charge, the larger discharge capacity than the theoretical value, the evolution of 3 V plateaus during the electrochemical cycling, and the disappearance of the XRD peaks corresponding to Li–Mn ordering in the transition-metal layers after extended cycling. These studies are currently under way and will be published elsewhere.

Acknowledgements

This work was supported by the US Department of Energy, FreedomCAR and Vehicle Technologies Program under contract No. W-31-109-ENG-38.

References

[1] K. Numata, S. Yamanaka, Solid State Ionics 118 (1999) 117.
[2] B. Ammundsen, J. Paulsen, Adv. Mater. 13 (2001) 943.
[3] Z. Lu, D.D. MacNeil, J.R. Dahn, Electrochem. Solid-State Lett. 4 (2001) A191.
[4] J.-S. Kim, C.S. Johnson, M.M. Thackeray, Electrochem. Commun. 4 (2002) 205.
[5] L. Zhang, H. Noguchi, J. Electrochem. Soc. 150 (2003) A601.
[6] V. Massarotti, M. Bini, D. Capsoni, A. Altomare, A.G.G. Moliterni, J. Appl. Cryst. 30 (1997) 123.
[7] Z. Lu, J.R. Dahn, J. Electrochem. Soc. 149 (2002) A815.
[8] S.-H. Kang, J. Kim, M.E. Stoll, D.A. Abraham, Y.-K. Sun, K. Amine, J. Power Sources 112 (2002) 41.
[9] S.-S. Shin, Y.-K. Sun, K. Amine, J. Power Sources 112 (2002) 634.
[10] S.-H. Kang, Y.-K. Sun, K. Amine, Electrochem. Solid-State Lett. 6 (2003) A183.
[11] J.-H. Kim, C.S. Yoon, Y.-K. Sun, J. Electrochem. Soc. 150 (2003) A538.
[12] Y.-K. Sun, M.-G. Kim, S.-H. Kang, K. Amine, J. Mater. Chem. 13 (2003) 319.
[13] L.A. Montoro, M. Abbate, J.M. Rosolen, J. Electrochem. Soc. 147 (2000) 1651.
[14] J.M. Rosolen, M. Abbate, Solid State Ionics 139 (2001) 83.
[15] W.-S. Yoon, K.-B. Kim, M.-G. Kim, M.-K. Lee, H.-J. Shin, J.-M. Lee, J.-S. Lee, C.-H. Yo, J. Phys. Chem. B 106 (2002) 2526.
[16] W.-S. Yoon, K.-B. Kim, M.-G. Kim, M.-K. Lee, H.-J. Shin, J.-M. Lee, J. Electrochem. Soc. 149 (2002) A1305.
[17] A.R. Armstrong, P.G. Bruce, Nature 381 (1996) 499.
[18] Y.-I. Jang, B. Huang, H. Wang, D.R. Sadoway, Y.-M. Chiang, J. Electrochem. Soc. 146 (1999) 3217.
[19] J.M. Paulsen, C.L. Thomas, J.R. Dahn, J. Electrochem. Soc. 147 (2000) 861.